Characterization of Surfaces with Sonars Using Time of Flight and Triangulation

Carlos Albores and José Luis Gordillo

Intelligent Systems Center, ITESM Campus Monterrey
Ave. Eugenio Garza Sada 2501 Sur, C. P. 64849
Monterrey, Nuevo León, México, Tel. (+52)(81)83284379
calbores@cia.mty.itesm.mx, JLGordillo@itesm.mx

Abstract. This paper presents a simple and original method that uses a configuration of only two sonars to measure and characterize surfaces. The method uses simultaneously the Time Of Flight (TOF) technique and basic triangulation, and characterizes the obtained sonar data into corners, edges and planes, along with non-classified points. The characterization is based on a simple trigonometric evaluation. A commutation system with two sonars that use a configuration with a transmitter and two receivers was built to verify the proposed methodology. Experiments and satisfactory results are also presented.

1 Introduction

Sonars are ultrasonic devices widely used in autonomous vehicles and robot navigation [1,2]. These sensors provide a cheap option to measure distances and to detect obstacles. The most common strategy used by sonars to obtain measurements is called Time Of Flight (TOF), which consists of sending an ultrasonic pulse and measuring the elapsed time until the echo returns after hitting an object. Although TOF measurement in several cases is simple and precise, its interpretation is difficult and tends to provide incorrect appreciations. An example of the results obtained by a sequence of readings with a rotating system of sonars (rotational scan) is shown in Figure 1, with the real environment superimposed. The modelling of a certain environment with only a set of straight and well-defined lines is difficult because some surfaces cannot be clearly detected. This fact provoked the abandonment of sonars as a sole medium of navigation [3]. In spite of this, some variants of the original TOF technique have recently proved to be useful in environment mapping and characterization. These variants are characterized by increasing the number of receiving sonars for each sonar emission. This approach obtains quite reliable measurements, thus better representations of the studied environment [4,5]. These works have been developed testing different quantities of receiving sonars (2 to 4) by one transmitting sonar. The transducers used as transmitters are activated one by one, but never at the same time. These methods are based on information redundancy obtained after activating all the transmitting sonars [6]. All of these investigations use more than two sonars. In addition, a system capable of distinguishing objects with

A. Sanfeliu and J. Ruiz-Shulcloper (Eds.): CIARP 2003, LNCS 2905, pp. 212–220, 2003.

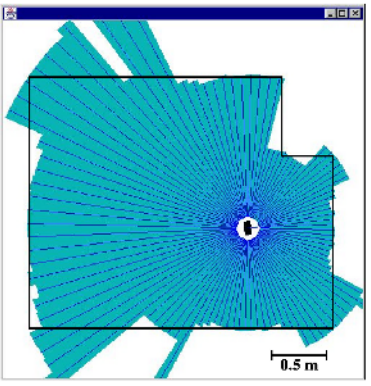

Fig. 1. Scan of a sonar, the real environment is superimposed for comparison.

a minimum of two transmitters and two receivers has been described [7]. This configuration uses three sonars: a sonar used exclusively as transmitter, another used exclusively as receiver, whereas the third one has a transmitter/receiver function. In all the previous methods, the characterization is based on complex probabilistic estimation.

This article describes a simple and cheap method for characterizing indoor environments. It consists of using two sonars simultaneously under a one transmitter and two receivers configuration, in such a manner that complementary TOF values are obtained. Using triangulation, these values allow us to classify the measurements in concave corners, edges, planes and non-classified points. The sonar configuration is similar to the used in [8], however, in our research, both sonars alternate the transmitting role. Thus, in this investigation the structures of interest were mainly polygonal indoor environments with right angles.

The proposed method is optimal in the sense that, in order to acheive triangulation, the minimum number of required sonars are used. At the same time, the characterization is based on a very simple trigonometric evaluation, whose equations are also provided in this paper.

Furthermore, a very cheap system of sonars was built to verify the method. The system only uses two Polaroid© 6500 modules to sense the environment.

This paper is organized as follows: Section 2 analyses the configuration with one transmitter and two receivers. In Section 3 some experiments and their results are shown. Finally, Section 4 presents the conclusions of this work.

2 A Commutated Transmitter with Two Receivers

The signal emmited by the sonars could behave in two different ways. If the dimension of the surfaces that produce echo is larger than the wavelength of the sonar, the signal will be reflected. Otherwise, the signal will be diffracted. The reflecting surfaces return the signal based on the law of reflection, causing

a specular reflection. Planes and corners are in this category. In contrast, the diffracting surfaces return the signal in all directions in a similar way to diffuse reflection, decreasing the echo signal very fast. In this category the edges are included.

Figure 2(a) describes the configuration used in this research. The commutating sonars (T_1 and T_2) are separated by a distance b. First, sonar T_1 transmits and both sonars (T_1 and T_2) receive the signal, obtaining two measurements ($r_{1\,1}$ and $r_{1\,2}$). Afterwards, sonar T_2 transmits and its signal is received by both sonars, obtaining other two measurements ($r_{2\,1}$ and $r_{2\,2}$). $r_{i\,j}$ is the distance obtained when sonar T_i transmits and sonar T_j receives. Therefore, the proposed plan of a transmitter and two receivers obtains four measurements to calculate the distance between the object and the sonars, which helps to classify the objects into concave or convex, as corners and edges, respectively.

Next, measurements in different surfaces are analyzed, in the following order: plane, corner and edge. To distinguish between these types of surfaces the relationship: $r_{1\,2} + r_{2\,1} - (r_{1\,1} + r_{2\,2})$ is analyzed and corresponds to the sum of the crossed distances (different transmitter than receiver) minus the direct distances (same transmitter and receiver). Moreover, in each case it will be derived the distance a which is the length from the center of the arrangement of sonars to the analyzed point, and the angle ϕ which is the angle between a and b's perpendicular line. These two variables represent the most accurate measurements that can be obtained for both distance and angle. This is shown in Figure 2(a). A more detailed description of the obtained equations is found in [9].

To validate these calculations, we assume that $r_{1\,2} = r_{2\,1}$, which establishes that, in an environment that does not change in time, and in which each sonar is found inside the other's range; the crossed distances (different transmitter than receiver) should be the same.

Finally, note that the sonars reflections are used in the plane and corner analysis [7] to make them easier.

Analyses of the three cases (*plane*, *corner* and *edge*) are presented in the next subsections.

2.1 Plane

In Figure 2(a) the reflections of the sonars are shown. Distances $r_{i\,j}$ represent the distance obtained from the sonar T_i to sonar T_j reflection (T'_j); for example, $r_{1\,1}$ goes from T_1 to T'_1.

Along with these distances, Figure 2(a) shows the following variables:

b**:** distance of T_1 to T_2. $b = |\mathbf{b}|$, where $\mathbf{b} = \overline{T_2 T_1}$.
a**:** distance between the medium point of $\mathbf{b}$ and the plane. $a = |\mathbf{a}|$, where $\mathbf{a}$ is the vector that goes from $\mathbf{b}$'s medium point to the plane.
$r_{i\,j}$**:** distance from T_i to T'_j. $r_{i\,j} = |\mathbf{r}_{i\,j}|$, where $\mathbf{r}_{i\,j} = \overline{T_i T'_j}$.
α_1**:** angle from $\mathbf{b}$'s perpendicular to $\mathbf{r}_{1\,1}$.
α_2**:** angle from $\mathbf{b}$'s perpendicular to $\mathbf{r}_{1\,2}$.
β**:** angle from $\mathbf{r}_{1\,1}$ to $\mathbf{r}_{1\,2}$.

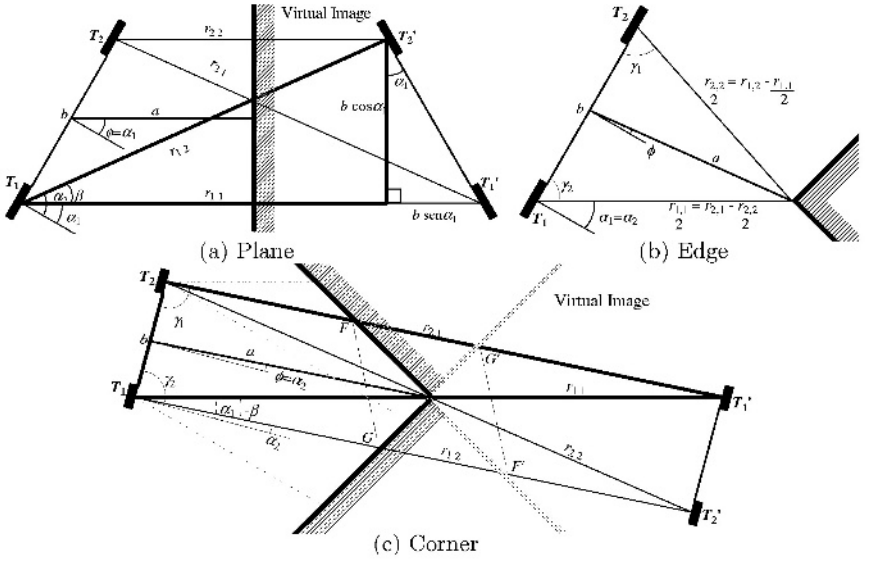

Fig. 2. Plane, Corner and Edge analysis. In (a) and (c) it is illustrated the reflection of both sonars over the wall (T_1' and T_2'). Besides, the four distances r are observed in all three cases.(based on [6]).

ϕ**:** angle from **b**'s perpendicular to **a**.

From these values we will deduce a, ϕ, and the behavior of $r_{1\,2} + r_{2\,1} - (r_{1\,1} + r_{2\,2})$.

According to Figure 2(a):

$$r_{1\,1} + r_{2\,2} = 4a, \tag{1}$$

from the triangle conformed by $r_{1\,2}$ and $b\cos\alpha_1$ it can be demonstrated that its base is equal to $2a$. Now, to determine the difference between $r_{1\,2} + r_{2\,1} - (r_{1\,1} + r_{2\,2})$, first $r_{1\,1}$ is derived,

$$r_{1\,1} = b\sin\alpha_1 + 2a, \tag{2}$$

of the right triangle is obtained:

$$r_{1\,2} = r_{2\,1} = \sqrt{4a^2 + b^2\cos^2\alpha_1}, \tag{3}$$

adding the crossed distances, considering $a >> b$, and rearranging some terms,

$$r_{1\,2} + r_{2\,1} = 2\sqrt{4a^2 + b^2\cos^2\alpha_1} \approx 4a\left(1 + \frac{b^2\cos^2\alpha_1}{8a^2}\right), \tag{4}$$

then, the relationship of the crossed and direct distances is obtained

$$r_{1\,2} + r_{2\,1} - (r_{1\,1} + r_{2\,2}) \approx \frac{b^2\cos^2\alpha_1}{2a}. \tag{5}$$

Finally, ϕ is obtained easily, since is equal to angle α_1,

$$\alpha_1 = \arcsin\left(\frac{r_{1\,1} - r_{2\,2}}{2b}\right). \tag{6}$$

As it is clearly observed in equation (5), the result is always positive and varies according to a and α_1, since b remains constant once it is defined.

2.2 Corner

Figure 2(c) describes the corner analysis. It is worth to mention that the analysis is valid only if the corner's angle is 90°. In Figure 2 a reflection is made, similar to the one performed for the plane, adding or modifying the following variables:

a**:** distance between the center of b and the corner's vertex. This definition changes in regard to the presented one in the previos section
γ_1**:** angle from $\mathbf{b}$ to $\mathbf{r}_{2\,1}$
γ_2**:** angle from $\mathbf{r}_{1\,2}$ to $-\mathbf{b}$

As the previous case, we will obtain a, ϕ and $r_{1\,2}+r_{2\,1}-(r_{1\,1}+r_{2\,2})$. a is defined as,

$$r_{1\,2}+r_{2\,1}=4a \tag{7}$$

$$r_{1\,2}=r_{2\,1}=2a \tag{8}$$

of the triangle formed by b, $r_{1\,1}$ and $r_{2\,1}$, and making use of the cosines law,

$$r_{1\,1}=\sqrt{r_{2\,1}^2+b^2-2r_{2\,1}b\cos\gamma_1} \tag{9}$$

from the Figure 2(c) $\gamma_1=\frac{\pi}{2}+\alpha_2$ is obtained. Using a variable change in (9) and the following identities: $\cos\left(\frac{\pi}{2}+\alpha\right)=-\sin\alpha$ and $r_{2\,1}=2a$,

$$r_{1\,1}=\sqrt{r_{2\,1}^2+b^2-2r_{2\,1}b\cos\left(\frac{\pi}{2}+\alpha_2\right)}\approx+\frac{b^2}{4a}+b\sin\alpha_2. \tag{10}$$

It also can be shown that:

$$r_{2\,2}\approx 2a+\frac{b^2}{4a}-b\sin\alpha_2 \tag{11}$$

using equation (11) in $r_{1\,2}+r_{2\,1}-(r_{1\,1}+r_{2\,2})$,

$$4a-\left(2a+\frac{b^2}{4a}+b\sin\alpha_2\right)-\left(2a+\frac{b^2}{4a}-b\sin\alpha_2\right)\approx-\frac{b^2}{2a}. \tag{12}$$

In agreement with equation (12), the result for the corners is always negative, varying according to a. Finally, in the Figure 2 is observed that $\phi=\alpha_2$. It is not possible to get a general equation for corners whose angle is different from 90° using the described analysis, because in those cases the relation $\left|\overline{GF}\right|=\left|\overline{GF'}\right|=\left|\overline{G'F}\right|=\left|\overline{G'F'}\right|$ is no longer true and it is not valid to use the sonars reflection.

2.3 Edge

The edge analysis will be based on Figure 2(b). In this case, it is not possible to use the reflection of the sonars or virtual image, because the distances are not conserved when the reflection is done. Due to the lack of virtual image, the distances observed in Figure 2(b) only represent half of the measurements $r_{1\,1}$ and $r_{2\,2}$.

For the convex corners case, it can be shown that $r_{1\,2}+r_{2\,1}-(r_{1\,1}+r_{2\,2})=0$, this is because

$$r_{1\,2}=r_{2\,1}=\frac{r_{1\,1}}{2}+\frac{r_{2\,2}}{2}. \tag{13}$$

Then a is obtained using the sinus law with the triangle formed by $\frac{r_{2\,2}}{2}$, $\frac{b}{2}$ and a, deriving

$$a = \sqrt{\left(\frac{r_{2\,2}}{2}\right)^2 + \left(\frac{b}{2}\right)^2 - \frac{r_{2\,2}b}{2}\cos\gamma_1}. \tag{14}$$

Finally, ϕ is obtained,

$$\phi = \frac{\pi}{2} - \cos^{-1}\left(\frac{\left(\frac{b}{2}\right)^2 + a^2 - \left(\frac{r_{2\,2}}{2}\right)^2}{ab}\right). \tag{15}$$

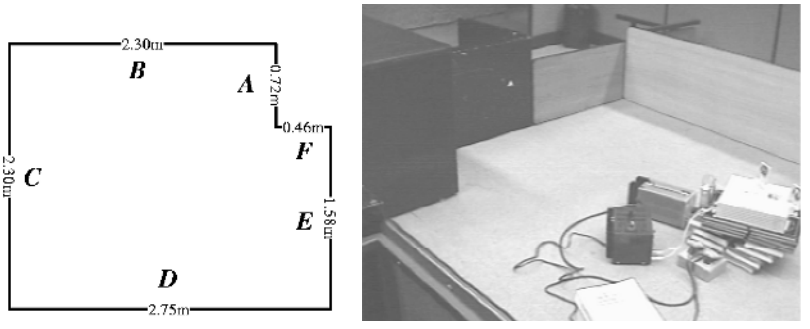

(a) Experiment environment (b) First view

Fig. 3. Experiment environment and different views of the designed environment and the experimental setup. In (a) each capital letter represents a line in the environment.

3 System Implementation and Experiments

To verify the theory described in this article a system with an arrangement of two sonars mounted on a rotating mechanism (see Figure 3) was built and a graphic interface was developed in JAVA to visualize, store and analyze the collected data. The system is composed of two Polaroid 6500 modules to control the sonar transducers.

The experimental environment is similar to that of an indoor robot. Views of the environment and its dimensions are illustrated in Figure 3.

The environment was built having in mind following considerations: First, The environment was built using a proper material to reflect adequately the sonar signal. Tables and desks of wood were used for this purpose. Besides, the surfaces should be flat and without holes.

The first experimental step consists in scanning the environment to obtain the readings. The system delays around two minutes to obtain a scan, and it senses 100 points in one scan (400 r distances). Then, the information is processed and its characterization is obtained. Examples of the results of this process are shown

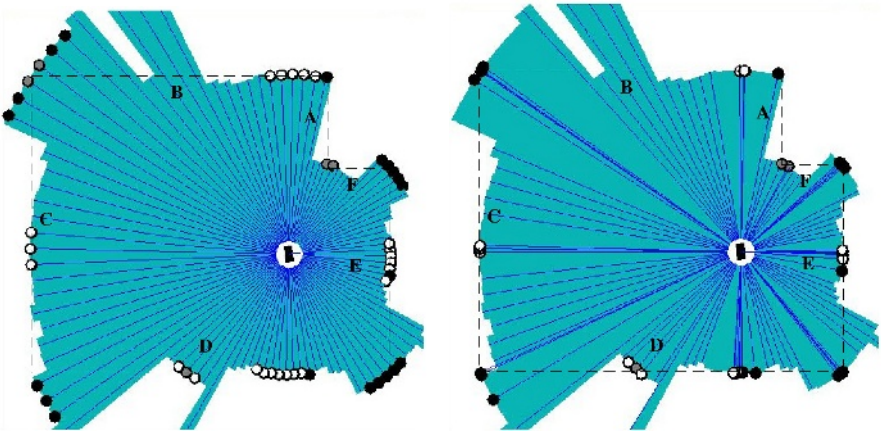

(a) Characterization **C1** (b) **C1** whit a and ϕ

Fig. 4. Scan characterizations from a given position. The points are characterized as follows: corners, black circles; planes, white and edges, gray. In (b) distance a and angle ϕ mentioned in the text are shown and represented by the lines that come out of the center of the figure. Non-classified points were assigned an omission value of $\phi = 0$ and don't have a circle to represent them. Real environment is shown in dashed lines.

in Figures 4(a) and 4(b). The circles are points that the system recognizes as corners, planes or edges. It is observed in the Figures that is difficult to detect the edges correctly. The dashed line in these Figures represents the real environment.

In contrast, it is observed in the Figures that not all the scan readings are classified as corners, edges, or planes. These are the non-classified points, due to:

1. The condition that the crossed distances must be equal ($r_{1\,2} = r_{2\,1}$) is not satisfied, probably because one sonar signal is not detected by the other (receiver).
2. One of the sonars or both are unable to detect the surfaces to be measured.
3. The sum of the crossed distances minus the sum of the direct distances does not correspond to any of the three cases afore mentioned.

As it is shown in Figure 4, the system has a detection level of more than 80% in corners and planes (in readings that should be characterized as such entities), but only reaches a level of 40% in edges, since they are very difficult to measure due to the diffraction of the echo. It is worth to mention that when a reading is considered as not classified, the system uses for analysis the smallest of the four r obtained in that point.

Note that Figure 4(a) show groups of readings mainly in the corners and planes of the real environment. In Figure 4(b) angle ϕ is used, and it is observed

how the characterized points converge in the corners and planes of the real environment.

This technique has advantages upon similar vision techniques, i.e. structured light or stereoscopic vision, mainly in the price and amount of information that is needed to process.

4 Conclusions

This investigation proposes a method that utilizes two sonars for the measurement and characterization of surfaces. The method is based on the combination of the TOF technique and triangulation, which applies basic trigonometry calculations to differentiate among corners, edges and planes.

The experiments were performed in an environment built up with tables and desks in order to validate and evaluate the behavior of the implemented System.

The System recognized corners and planes correctly, but edges were more difficult.

The system proved to be reliable and efficient . In addition, the system is very cheap, no expensive hardware is required.

The system could be improved, specially in regards to noise problems with sonars, characterization of discontinued segments and verification of erroneous segments generated by data segmentation.

Finally, based on the obtained results we conclude that the proposed method is reliable when used in environments complying with the requisites afore mentioned. In addition, this research leaves a solid base for future jobs that require sonar systems. For example, the system can be included in robots and autonomous vehicles that require a more precise, cheap and reliable environment modelling for a better navigation.

References

1. Leonard, J., Durrant-Whyte, H.: Simultaneous map building and localization for an auotonomous mobile robot. In: IEEE International Workshop on Intelligent Robots and Systems. Volume 3. (1991) 1442–1447
2. Jensfelt, P.and Austin, D.W.O.A.M.: Feature based condensation for mobile robot localization. In: IEEE International Conference on Robotics and Automation. Volume 3. (2000) 2531–2537
3. Kuc, R.: A spatial sample criterion for sonar obstacle detection. IEEE Transactions on Pattern Analysis and Machine Intelligence **12** (1990) 686–690
4. Arikan, O., Barshan, B.: A comparison of two methods for fusing information from a linear array of sonar sensors for obstacle localization. In: International Conference on Intelligent Robots and Systems. Volume 2. (1995) 536–541
5. Hong, M.L., Kleeman, L.: A low sample rate 3D sonar sensor for mobile robots. In: IEEE International Conference on Robotics and Automation. Volume 3. (1995) 3015–3020

6. Barshan, B., Kuc, R.: Differentiating sonar reflections from corners and planes by employing an intelligent sensor. IEEE Transactions on Pattern Analysis and Machine Intelligence **12** (1990) 560–569
7. Kleeman, L., Kuc, R.: Mobile robot sonar for target localization and clasification. The International Journal of Robotics Research **14** (1995) 295–318
8. Manyika, J., Durrant-Whyte, H.: A tracking sonar sensor for vehicle guidance. In: IEEE. Volume 3. (1993) 424–429
9. Albores, C.: Sistema de sonares para la localización y caracterización de superficies 2-D usando tiempo de vuelo y triangulación. Master's thesis, Instituto Tecnológico y de Estudios Superiores de Monterrey, Campus Monterrey (2001) in spanish.